Simple Fully Analytical Copper Loss Model of Litz Wire Made of Strands Twisted in Multiple Levels

Kazuhiro Umetani
Graduate school of natural science and technology
Okayama University
Okayama, Japan
umetani@okayama-u.ac.jp

Jesús Acero
Department of Electronic Engineering and Communications
University of Zaragoza
Zaragoza, Spain
jacero@unizar.es

Héctor Sarnago
Department of Electronic Engineering and Communications
University of Zaragoza
Zaragoza, Spain
hsarnago@unizar.es

Óscar Lucia
Department of Electronic Engineering and Communications
University of Zaragoza
Zaragoza, Spain
olucia@unizar.es

Eiji Hiraki
Graduate school of natural science and technology
Okayama University
Okayama, Japan
hiraki@okayama-u.ac.jp

***Abstract*— The Litz wire has been widely utilized as a wire with a low copper loss under high-frequency operation. However, design optimization of the Litz wire is difficult because this wire generally has a complicated structure of thin strands twisted in multiple levels, which hinders both of the analytical and numerical prediction of the copper loss. To overcome this issue, recent studies have proposed the analytical models of the copper loss in the bundle of twisted strands, which is the basic components constituting the Litz wire. This paper constructs a simple analytical copper loss model of the Litz wire based on these preceding insights. In addition to these insights, the proposed model further considers the effect of the inclination angle of the strands to the Litz wire on the proximity effect loss. The proposed model was tested in comparison with the experimentally measured AC resistance of commercially available Litz wires. As a result, the predicted AC resistance showed good agreement with the measured ac resistance, suggesting the effectiveness of the proposed model.**

Keywords—AC resistance, analytical model, copper loss, Litz wire, proximity effect

I. INTRODUCTION

The Litz wire is widely utilized in industrial applications that require high-frequency AC power, such as induction heating [1]–[3] and high-frequency resonant converters [4]–[8]. The Litz wire is made of a number of thin strands twisted in multiple levels, e.g. the twisted bundles each made of twisted strands. As pointed out in [9][10], twisting the strands can prevent concentration of the ac current in particular strands. Therefore, the complicated structure of the Litz wire with multi-level twisting can ensure equal ac current flows among all the strands constituting the Litz wire. As a result, the Litz wire can effectively suppress the copper loss even under high-frequency operation.

However, the too many levels of twisting may result in an increase in manufacturing cost and decrease the packing factor, which expands the volume occupied by the wire. Therefore, the design of the Litz wire commonly requires seeking effective suppression of the copper loss with simple twisting structure.

In this sense, efficient design of the Litz wire may need a prediction of the copper loss from the geometrical specifications of the Litz wire, such as the twisting structure, the diameter, and the number of the strands. However, the copper loss prediction of the Litz wire has been regarded to be difficult both for the analytical and numerical [11]–[14] approaches because multi-level twisting of many thin strands generally requires complicated modeling based on the electromagnetic analysis.

Preceding studies [15]–[25] have proposed analytical prediction methods of the copper loss in the bundle of twisted strands (or the Litz wire with a single level of twisting), which is the basic element of the Litz wire. These methods provide analytical models of the skin and proximity effect of the bundle. Some of these models even have attractive features that they contain only physical constants and geometrical parameters, all of which can be straightforwardly obtained without FEM analysis. Therefore, the copper loss model of the Litz wire may be constructed by further considering the twisting process of these bundles.

The purpose of this paper is to construct a simple copper loss model based on these preceding insights. In addition to these insights, the proposed model further considers the effect of the inclination angle of the strands to the Litz wire, caused through the twisting process. The proposed model applies drastic approximations to simplify the equation so that only physical constants and geometrical parameters are required for the copper loss prediction.

The following discussion comprises 4 sections. Section II analytically derives the copper loss model of the Litz wire. In this section, we first briefly review the analytical copper loss model of the strand. Then, we derive the analytical copper loss model of the bundle of the twisted strands. As a result of the detailed analytical discussions, we propose a slight modification of the previous copper loss model of the bundle proposed in [25]. Based on the model of the bundle, we construct the copper loss model of the Litz wire. Section III presents experiments performed to verify the proposed copper loss model of the Litz wire. Finally, section IV gives conclusions.

II. COPPER LOSS MODEL OF LITZ WIRE

This section derives an analytical copper loss mode based on an example of a typical Litz wire, illustrated in Fig. 1, carrying sinusoidal ac current. This Litz wire has 3 levels of the twisting. As in many commercially available Litz wires, this Litz wire (3rd level bundle) is assumed to be formed by twisting no more than 5 bundles (2nd level bundle), each of which is formed by twisting no more than 5 bundles (1st level

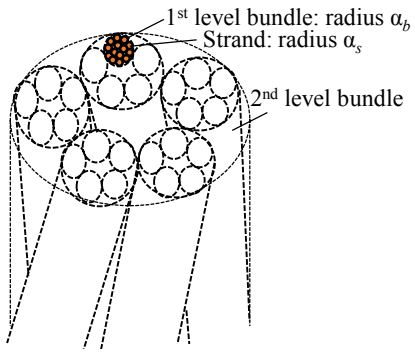

Fig. 1. Litz wire structure under consideration with 3 levels of twisting.

bundle). However, 1st level bundles are assumed to be formed by twisting many (much more than 5) strands, as is common in many Litz wire.

The copper loss of a wire is generally dependent on two factors: One is the ac current flowing through the wire, and the other is the external ac magnetic field applied to the wire. Therefore, the copper loss model should be expressed as a function of these two factors. The Litz wire under consideration is assumed to carry the total ac current i_L. In addition, the uniform sinusoidal external ac magnetic field $\mathbf{H}_L$ is assumed to be applied in perpendicular to the Litz wire.

Derivation of the proposed copper loss model is based on modeling of the copper loss in each level of twisting in the Litz wire. We first derive the analytical copper loss model of a strand. Then, based on this model of the strand, we formulate the analytical copper loss model of a bundle made of the strands. Finally, we formulate the analytical copper loss model of the Litz wire based on the model of the bundle. Because the Litz wire is made of non-magnetic material, the linear media is assumed in the electromagnetic analysis.

A. Analytical Copper Loss Model of Strand

We focus on a strand shown in Fig. 2 and formulate the copper loss of the strand. The strand is assumed to carry the ac current i_s. In addition, the external ac magnetic field $\mathbf{H}_s$ is applied to the strand, although we do not limit the direction of $\mathbf{H}_s$ to be perpendicular to the strand.

The copper loss of the strand is the sum of the Joule loss generated by the local ac current inside the strand. Therefore, the copper loss of the unit length of the strand P_s can be expressed as

$$P_s = \int_{S_s} \rho \left| \mathbf{i}_{s\_dens} \right|^2 dS_s , \tag{1}$$

where ρ is the resistivity of the copper, S_s is the horizontal cross-section of the strand, and $\mathbf{i}_{s\_dens}$ is the local ac current density vector inside the strand.

The local ac current density is the sum of the eddy current density, generated by $\mathbf{H}_s$, and the ac current density $\mathbf{i}_{acs\_dens}$, constituting i_s under the absence of the external field. We denote the component of $\mathbf{H}_s$ in perpendicular and in parallel to the strand as $\mathbf{H}_{s\perp}$ and $\mathbf{H}_{s//}$, respectively. Then, (1) can be rewritten as

$$P_s = \int_{S_s} \rho \left| \mathbf{i}_{acs\_dens} + \mathbf{i}_{s\perp\_dens} + \mathbf{i}_{s//\_dens} \right|^2 dS_s , \tag{2}$$

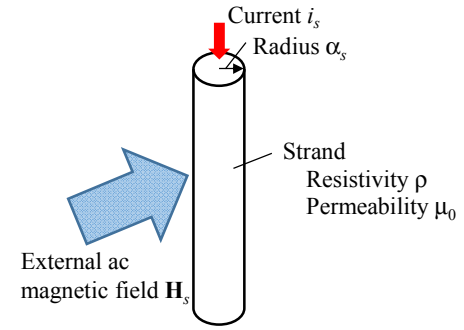

Fig. 2. Strand under consideration.

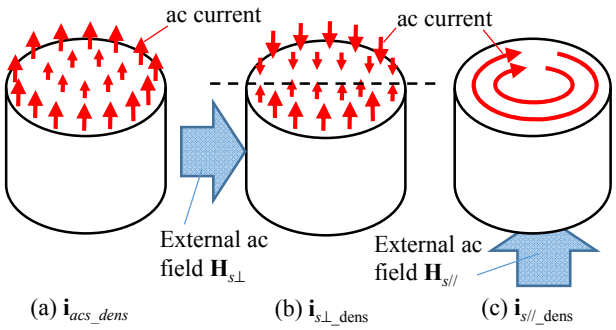

Fig. 3. AC current distributions of the ac current density $\mathbf{i}_{acs\_dens}$, which constitutes i_s under the absence of the external field, and the eddy current $\mathbf{i}_{s\perp\_dens}$ and $\mathbf{i}_{s//\_dens}$, which is generated by $\mathbf{H}_{s\perp}$ and $\mathbf{H}_{s//}$, respectively.

where $\mathbf{i}_{s\perp\_dens}$ and $\mathbf{i}_{s//\_dens}$ is the eddy current generated by $\mathbf{H}_{s\perp}$ and $\mathbf{H}_{s//}$, respectively.

As depicted in Fig. 3, the current density $\mathbf{i}_{acs\_dens}$ and $\mathbf{i}_{s\perp\_dens}$ are in parallel to the strand, whereas $\mathbf{i}_{s//\_dens}$ is in perpendicular to the strand. Furthermore, $\mathbf{i}_{acs\_dens}$ has the axial symmetry with respect to the central axis of the strand, whereas $\mathbf{i}_{s\perp\_dens}$ has the anti-symmetry with respect to the line passing through the center of the strand and in parallel to $\mathbf{H}_{s\perp}$ (dashed line in Fig. 3(b)). Noting that $\mathbf{i}_{s\perp\_dens}$ and $\mathbf{i}_{s//\_dens}$ must be proportional to the magnitude of $\mathbf{H}_{s\perp}$ and $\mathbf{H}_{s//}$, respectively, in the linear media, we can further express (2) as

$$\begin{aligned} P_s &= \rho \int_{S_s} \left| \mathbf{i}_{acs\_dens} \right|^2 dS_s + \rho \int_{S_s} \left| \mathbf{i}_{s\perp\_dens} \right|^2 dS_s \\ &\quad + \rho \int_{S_s} \left| \mathbf{i}_{s//\_dens} \right|^2 dS_s , \\ &= R_s i_s^2 + G_{s\perp} H_{s\perp}^2 + G_{s//} H_{s//}^2 \end{aligned} \tag{3}$$

where R_s is the strand-level loss coefficient caused by the skin effect; $G_{b\perp}$ and $G_{b//}$ are the proximity effect coefficients, respectively.

According to the preceding studies [15]–[25], these coefficients are analytically derived as

$$R_s = \frac{\rho}{\pi \alpha_s^2} F(\gamma_s), \tag{4}$$

$$G_{s\perp} = 4\pi\rho K(\gamma_s), \tag{5}$$

$$G_{s//} = 2\pi\rho K(\gamma_s), \tag{6}$$

where α_s is the radius of the strand. Parameter γ_s and functions F and K are defined as

$$\gamma_s \equiv \alpha_s \sqrt{\frac{\omega \mu_0}{\rho}}, \tag{7}$$

$$F(x) \equiv \frac{x}{2} \frac{\mathrm{ber}\, x\, \mathrm{bei}' x - \mathrm{ber}' x\, \mathrm{bei}\, x}{(\mathrm{ber}' x)^2 + (\mathrm{bei}' x)^2}, \tag{8}$$

$$K(x) \equiv -x \frac{\mathrm{ber}_2\, x\, \mathrm{ber}' x + \mathrm{bei}_2\, x\, \mathrm{bei}' x}{(\mathrm{ber}\, x)^2 + (\mathrm{bei}\, x)^2}, \tag{9}$$

where ω is the angular frequency, μ_0 is the permeability of the air.

B. Analytical Copper Loss Model of 1st Level Bundles

A 1st level bundle is a group of twisted strands. Therefore, the strands placed at the same distance from the center of the bundle rotationally exchange their position along the bundle. This indicates that these strands must carry the same ac current. Hence, the current distribution among the strands of the 1st level bundle must have the axial symmetry.

As mentioned in the previous subsection, the external magnetic field applied in perpendicular to the bundle must induce the ac current with the anti-symmetry distribution with respect to the line passing through the center of the bundle and in parallel to the field. However, this anti-symmetry current distribution cannot be achieved in the 1st level bundle because of the requirement of the axial symmetry current distribution among the strands. As a result, this external magnetic field does not induce the ac current circulating through any pairs of the strands, although this field still induces the local eddy current confined inside the strand, i.e. $\mathbf{i}_{s\perp\_dens}$ mentioned in the previous subsection. (We neglected the bundle-level proximity effect [25] because we assume the Litz wire much longer than the twisting pitch.)

Similarly, the external magnetic field applied in parallel to the bundle must induce the ac current of the direction in perpendicular to the bundle. However, the bundle is made of thin isolated strands; and therefore, this requirement cannot also be achieved in the bundle. As a result, this external magnetic field does not induce the circulating ac current through the strands, although this field still induces the local eddy current inside the strands, i.e. $\mathbf{i}_{s//\_dens}$.

Consequently, the copper loss per unit length of the 1st level bundle P_b has the following form.

$$P_b = R_b i_b^2 + \sum_j G_{s\perp} H_{s\perp j}^2 + \sum_j G_{s//} H_{s// j}^2 \tag{10}$$

where R_b is the bundle-level loss coefficient caused by the strand-level and bundle-level skin effect; i_b is the total ac current flowing through the bundle; j is the index of the strands contained in this 1st level bundle; $H_{s\perp\mathrm{j}}$ and $H_{s//\mathrm{j}}$ are the RMS value of the local external magnetic field $\mathbf{H}_{s\perp}$ and $\mathbf{H}_{s//}$, respectively, at the strand j.

The coefficient R_b can be regarded as the ac resistance of the bundle under the absence of the external magnetic field. Therefore, we can determine R_b by calculating the copper loss when no external magnetic field is applied to the bundle. Note that the electromagnetic field of the bundle-level must have the axial symmetry inside the bundle because the current distribution among the strands in the bundle also has the axial symmetry. In this case, we can approximate the ac current distribution among the strands in the bundle as the ac current distribution inside the solid wire with the same diameter as the bundle.

We assume that this imaginary solid wire is made of the uniform material with the resistivity ρ_{eff} defined as

$$\rho_{eff} = \frac{A_s}{\eta} R_s \tag{11}$$

where η is the porosity factor of the bundle, and A_s is the cross-sectional area of the strand. This solid wire model gives the solution of the ac current distribution that ensures 1. the direction of the ac current to be in parallel to the bundle and 2. the ac electric potential to be the same at any point inside the cross-section of the solid wire. If we assume the same ac current distribution inside the bundle as the solid wire, we can find that these features satisfy the requirement of the ac current distribution among the strands in the bundle because

1. The former feature prohibits the ac current flowing outside the strand, (We assume that the inclination angle of the strands to the bundle is small because the diameter of the 1st level bundle is far smaller than that of the Litz wire and therefore twisting the strands does not cause large inclination angle to the bundle.)
2. The latter feature prohibits the ac current circulating through any pair of the strands.

Furthermore, the total copper loss generated in this solid wire model is the same as the copper loss in the bundle. In fact, by determining the strand current i_s according to

$$i_s = \frac{A_s}{\eta} i_{b\_dens}, \tag{12}$$

where i_{b_dens} is the ac current density vector component parallel to the wire in the solid wire model (The component perpendicular to the wire is zero.), we have

$$i_b = \sum_j i_s = \frac{A_s}{\eta} \sum_j i_{b\_dens} \approx \int_{S_b} i_{b\_dens} dS_b, \tag{13}$$

$$\begin{aligned} R_b i_b^2 &= \sum_j R_s i_s^2 = R_s \left(\frac{A_s}{\eta} \right)^2 \sum_j i_{b\_dens}^2 \\ &= \frac{A_s}{\eta} \sum_j \rho_{eff} i_{b\_dens}^2 \approx \int_{S_b} \rho_{eff} i_{b\_dens}^2 dS_b, \end{aligned} \tag{14}$$

Equation (13) indicates that the total ac current flowing through the bundle is the same as that in the solid wire model. In addition, (14) indicates that the total copper loss inside the bundle is the same as that in the solid wire model.

Therefore, the copper loss in the solid wire model can be analytically calculated, similarly as in the previous section. As a result, inferred from (4), R_b can be obtained as

$$R_b = \frac{\rho_{eff}}{\pi\alpha_b^2} F(\gamma_b) = \frac{A_s F(\gamma_b)}{\eta\pi\alpha_b^2} R_s, \quad (15)$$

where α_b is the radius of the 1st level bundle. Parameter γ_b is defined as

$$\gamma_b \equiv \alpha_b \sqrt{\frac{\omega\mu_0}{\rho_{eff}}}, \quad (16)$$

Substituting (4) into (15), R_b can be finally determined as

$$R_b = \frac{\rho}{\eta\pi\alpha_b^2} F(\gamma_s) F(\gamma_b) = \frac{\rho}{\pi\alpha_s^2 n_s} F(\gamma_s) F(\gamma_b), \quad (17)$$

where n_s is the number of the strand in a 1st level bundle.

The analytical solution of R_b, shown in (17), is similar to the model of the preceding study [25]. However, there is a slight difference that ρ_{eff} contained in γ_b was set at ρ/η in [25], whereas ρ_{eff} is defined as (11) in the proposed model. This difference may have a subtle effect on the calculation of R_b in many actual cases. Nonetheless, as discussed above, (17) has the theoretical basis on the electromagnetism.

C. Analytical Copper Loss Model of Litz Wire

The 2nd and 3rd level bundles are assumed to be formed by twisting no more than 5 bundles. Therefore, the bundles of the same twisting group rotationally exchange their position along the Litz wire. Because these bundles have the axial symmetry, thus carrying the same ac current. As a result, all of the 1st level bundles in the Litz wire carry the same ac current.

Noting that the 1st level bundles have a greater length than the Litz wire as a result of the twisting process, the total copper loss of the Litz wire P_L can be obtained as

$$P_L = mn_2n_1R_b\left(\frac{i_L}{n_2n_1}\right)^2 + mG_{s\perp}\sum_{k,j} H_{s\perp kj}^2 + mG_{s//}\sum_{k,j} H_{s//kj}^2, \quad (18)$$

where m is the length ratio of the 1st level bundle to the Litz wire, i_L is the total ac current of the Litz wire, n_1 is the number of the 1st level bundles in a 2nd level bundle, n_2 is the number of the 2nd level bundles in a Litz wire, and k is the index of the 1st level bundles contained in the Litz wire, $H_{s\perp kj}$ and $H_{s//kj}$ are the RMS value of the local external magnetic field $\mathbf{H}_{s\perp}$ and $\mathbf{H}_{s//}$, respectively, at the strand j in the 1st level bundle k.

Equation (18) still contains the unknown parameters $H_{s\perp kj}$ and $H_{s//kj}$. The next subsection discusses the derivation of these parameters to determine the copper loss model of the Litz wire.

D. Magnetic Field in Litz Wire

The multi-level twisting structure of Litz wire makes complicated the estimation of $H_{s\perp kj}$ and $H_{s//kj}$ because the strands have the inclination angle to the Litz wire. For example, the ac current flowing inside a bundle forms a circulating component around the center of the bundle. This current generates the magnetic field parallel to the bundle, as illustrated in Fig. 4, which does not appear without twisting.

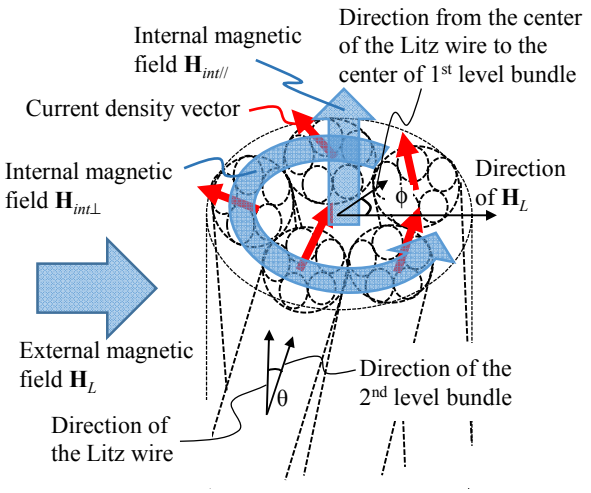

Fig. 4. Internal magnetic field genreated as a result of twisting.

This effect takes place in all levels of the twisting. However, considering this effect for all levels of bundles may lead to the extremely complicated calculation. Therefore, we simply consider this effect only for twisting the 2nd level bundles to form the Litz wire because its largest scale of twisting tends to be the major cause of the inclination angle of the strands. Hence, all the strands are assumed to be twisted to form the 1st level bundle with a negligible inclination angle to this bundle; and similarly, all the 1st level bundles are assumed to be twisted to form the 2nd level bundle with a negligible inclination angle to this 2nd level bundle. Nonetheless, all the 2nd level bundles are twisted with the constant inclination angles to the Litz wire. As a result, all the strands contained in a 2nd level bundle (and therefore all the strands of the Litz wire because of the axial symmetry among the 2nd level bundles) are assumed to be inclined at the same angle as the 2nd level bundle.

Because all the 1st level bundles carry the same ac current, we approximate the magnetic field inside the Litz wire as the sum of the external field $\mathbf{H}_L$ and the internal field $\mathbf{H}_{int}$ generated by the uniform current density in the Litz wire cross-section, flowing at the constant inclination angle θ. Certainly, the current distribution inside the 1st level bundles may not be uniform in high frequency due to the bundle-level skin effect, i.e. the ac current distribution of the solid wire model in subsection 2.B. However, we consider this small-scaled fluctuation of the magnetic field caused by this non-uniformity inside the 1st level bundle to be small compared with large-scale magnetic field generated by uniform current distribution among all the 1st level bundles.

Under this approximation, the internal magnetic field $\mathbf{H}_{int}$ can be determined as

$$H_{int//} = \frac{(a_L - r)\tan\theta}{\pi a_L^2} i_L, \quad (19)$$

$$H_{int\perp} = \frac{r}{2\pi a_L^2} i_L, \quad (20)$$

where $H_{int//}$ and $H_{int\perp}$ are the RMS values of the parallel and perpendicular components of $\mathbf{H}_{int}$ with respect to the Litz wire, a_L is the radius of the Litz wire, and r is the distance from the center of the Litz wire.

Because all the strands are assumed to be inclined to the Litz wire at the constant angle θ, the magnetic field at the strands can be obtained as

$$H_{s//kj}^2 = \left(-H_L \sin\phi_{kj} \sin\theta + H_{int\perp} \sin\theta + H_{int//} \cos\theta\right)^2, \tag{21}$$

$$H_{s\perp kj}^2 = \left(-H_L \sin\phi_{kj} \cos\theta + H_{int\perp} \cos\theta - H_{int//} \sin\theta\right)^2 + {H_L}^2 \cos^2\phi_{kj}, \tag{22}$$

where H_L is the RMS value of the external field and ϕ_{kj} is the angle between $\mathbf{H}_L$ and the vector drawn from the center of the Litz wire to the center of the strand j of the 1st level bundle k.

Therefore, the second and third terms of the right-hand side of (18) can be obtained by utilizing (19)–(22). First, we approximate the second and third terms by replacing the summation by the areal integration:

$$\begin{aligned} mG_{s\perp}\sum_{k,j} H_{s\perp kj}^2 &\approx mG_{s\perp}\frac{n_s n_1 n_2}{A_L}\int_{S_L} H_{s\perp kj}^2 dS_L \\ &= mG_{s\perp}\frac{n_{total}}{A_L}\int_{\phi_{kj}=0}^{2\pi} d\phi_{kj}\int_{r=0}^{a_L} rH_{s\perp kj}^2 dr, \end{aligned} \tag{23}$$

$$\begin{aligned} mG_{s//}\sum_{k,j} H_{s//kj}^2 &\approx mG_{s//}\frac{n_s n_1 n_2}{A_L}\int_{S_L} H_{s//kj}^2 dS_L \\ &= mG_{s//}\frac{n_{total}}{A_L}\int_{\phi_{kj}=0}^{2\pi} d\phi_{kj}\int_{r=0}^{a_L} rH_{s//kj}^2 dr, \end{aligned} \tag{24}$$

where n_s is the number of the strands in the 1st level bundles, and n_{total} is the total number of the strands contained inside the Litz wire (Hence, $n_{total}=n_s n_1 n_2$.), A_L is the cross-section area of the Litz wire, S_L is the horizontal cross-section of the Litz wire.

Substituting (19)–(22) into (23) and (24), we have

$$mG_{s\perp}\sum_{k,j} H_{s\perp kj}^2 \approx mG_{s\perp}n_{total}\left\{\frac{H_L^2}{2}\left(1+\cos^2\theta\right) + \left(\frac{1}{3\cos^2\theta}+\frac{11\cos^2\theta}{12}-1\right)\frac{i_L^2}{2\pi^2 a_L^2}\right\}, \tag{25}$$

$$mG_{s//}\sum_{k,j} H_{s//kj}^2 \approx mG_{s//}n_{total}\left(\frac{H_L^2}{2}+\frac{11}{24}\frac{i_L^2}{\pi^2 a_L^2}\right)\left(1-\cos^2\theta\right). \tag{26}$$

Because all the 1st level bundles are regarded to have the constant inclination angle θ to the Litz wire, the following relation is obtained between θ and m, i.e. the length ratio of the 1st level bundle to the Litz wire:

$$m = \frac{1}{\cos\theta}. \tag{27}$$

Substituting (27) into (25) and (26), we have

$$mG_{s\perp}\sum_{k,j} H_{s\perp kj}^2 \approx G_{s\perp}n_{total}\left\{\frac{H_L^2}{2}\left(m+\frac{1}{m}\right) + \left(\frac{m^3}{3}+\frac{11}{12m}-m\right)\frac{i_L^2}{2\pi^2 a_L^2}\right\}, \tag{28}$$

$$mG_{s//}\sum_{k,j} H_{s//kj}^2 \approx G_{s//}n_{total}\left(\frac{H_L^2}{2}+\frac{11}{24}\frac{i_L^2}{\pi^2 a_L^2}\right)\left(m-\frac{1}{m}\right). \tag{29}$$

Finally, analytical copper loss model of the Litz wire is obtained by substituting (17), (28), and (29) into (18)

$$\begin{aligned} P_L &= mn_2 n_1 \frac{\rho}{\pi\alpha_s^2 n_s}F(\gamma_s)F(\gamma_b)\left(\frac{i_L}{n_2 n_1}\right)^2 \\ &\quad + 4\pi\rho K(\gamma_s)n_{total}\left\{\frac{H_L^2}{2}\left(m+\frac{1}{m}\right) + \left(\frac{m^3}{3}+\frac{11}{12m}-m\right)\frac{i_L^2}{2\pi^2 a_L^2}\right\} \\ &\quad + 2\pi\rho K(\gamma_s)n_{total}\left(\frac{H_L^2}{2}+\frac{11}{24}\frac{i_L^2}{\pi^2 a_L^2}\right)\left(m-\frac{1}{m}\right), \\ &= \frac{m\rho}{\pi\alpha_s^2 n_{total}}F(\gamma_s)F(\gamma_b)i_L^2 \\ &\quad + \frac{4\pi\rho n_{total}K(\gamma_s)}{8\pi^2 a_L^2}\left(\frac{4m^3}{3}-\frac{13}{6}m+\frac{11}{6m}\right)i_L^2 \\ &\quad + 4\pi\rho n_{total}K(\gamma_s)\left(\frac{3m}{4}+\frac{1}{4m}\right)H_L^2, \end{aligned} \tag{30}$$

As can be seen in (30), the copper loss of the Litz wire can be expressed in the form of $P_L=R_L i_L^2+G_L H_L^2$, where R_L and G_L are the loss coefficient of the skin effect and that of the proximity effect. These coefficients are given as

$$\begin{aligned} R_L &= \frac{m\rho}{\pi\alpha_s^2 n_{total}}F(\gamma_s)F(\gamma_b) \\ &\quad + \frac{4\pi\rho n_{total}K(\gamma_s)}{8\pi^2 a_L^2}\left(\frac{4m^3}{3}-\frac{13}{6}m+\frac{11}{6m}\right), \end{aligned} \tag{31}$$

$$G_L = 4\pi\rho n_{total}K(\gamma_s)\left(\frac{3m}{4}+\frac{1}{4m}\right), \tag{32}$$

TABLE I. SPECIFICATIONS OF EXPERIMENTAL LITZ WIRES

	Wire A	Wire B
Strand diameter α_s	ϕ0.05mm	ϕ0.071mm
Litz wire diamter α_L	ϕ2.25mm	ϕ2.8mm
Number of strands n_{total}	1050	800
Wire length	3	3
Parameters n_s, n_1, n_2	42, 5, 5	40, 5, 4
Parameter m	1.055	1.077

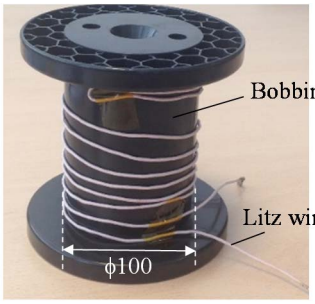

(a) Solenoidal coil for evaluation of R_L

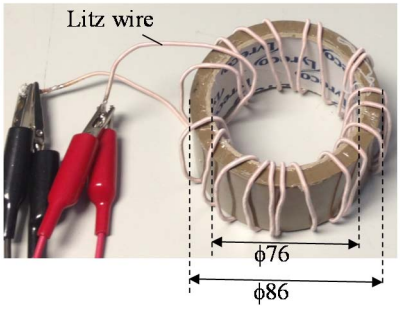

(b) Toroidal coil for evaluation of G_L

Fig. 5. Photographs of the experimental setup for evaluation of the loss coefficient R_L and G_L.

The proposed copper loss model of the Litz wire contains only physical constants and geometrical parameters of the Litz wire except for the external field H_L, which is dependent on the magnetic structure outside of the Litz wire and therefore should be given by the external condition. Therefore, the proposed model is a fully analytical copper loss model of the Litz wire.

III. EXPERIMENT

A simple experiment was carried out to verify the proposed copper loss model. In this experiment, we evaluated the copper loss coefficients R_L and G_L of two different Litz wires and compared the results with the theoretical values analytically calculated based on (31) and (32). These experimental Litz wires are formed with three levels of twisting. Specifications of these Litz wires are presented in Table I.

For the evaluation of R_L, the Litz wire to be tested was wound on the core-less bobbin to form a non-inductive solenoidal coil with four clockwise turns and four counter-clockwise turns, as shown in Fig. 5(a), so that the wire experience no external field H_L. The diameter of the bobbin was ϕ100mm. Then, we measured the frequency dependence of the ac resistance below 2MHz using the LCR meter

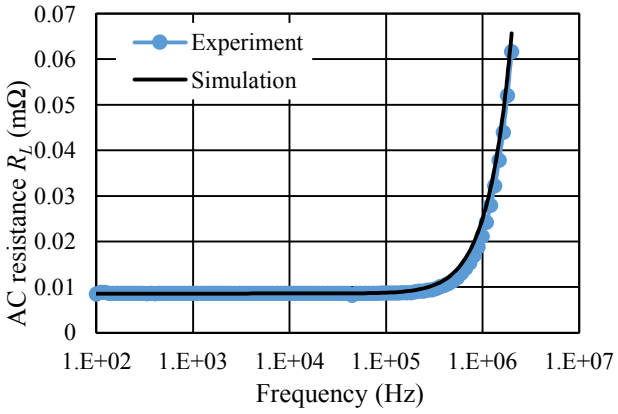

(a) Wire A

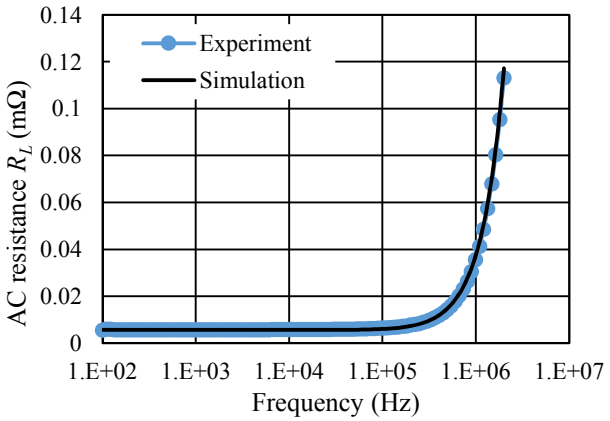

(b) Wire B

Fig. 6. Comparison result between the theoretically predicted R_L and experimentally measured R_L.

(Agilent E4980A). The measured ac resistance was divided by the total wire length to obtain the ac resistance per unit length, which equals R_L. Consequently, the frequency dependence of R_L was obtained as a result of this experiment.

For the evaluation G_L, the Litz wire to be tested was wound on the core-less toroid with 20 turns, as shown in Fig. 5(b), to generate the uniform ac magnetic field perpendicular to the wire. The inner and outer diameter of this toroid was ϕ76mm and ϕ86mm, respectively; and the height of the toroid was 50mm. Then, the frequency dependence of the ac resistance was measured below 2MHz using the LCR meter. The measured ac resistance was divided by the total wire length to obtain the ac resistance per unit length. The difference of the resultant ac resistance per unit length from R_L, which was measured using the non-inductive solenoidal coil, is the ac resistance per length contributed by the external ac magnetic field. Therefore, we compared this ac resistance difference with the theoretical value to verify G_L of the proposed model.

We denote this ac resistance difference per unit length as R_{GL}. The theoretical value of R_{GL} can be obtained as follows. The ac magnetic field inside the toroidal Litz wire coil H_{troid} can be approximately calculated as

$$H_{troid} = \frac{Ni_L}{2\pi r_{eq}}, \tag{33}$$

where N is the number of turns wound on the toroid, and r_{eq} is the representative distance from the center of the toroid to the coil. In this experiment, we simply set r_{eq}=40.5mm,

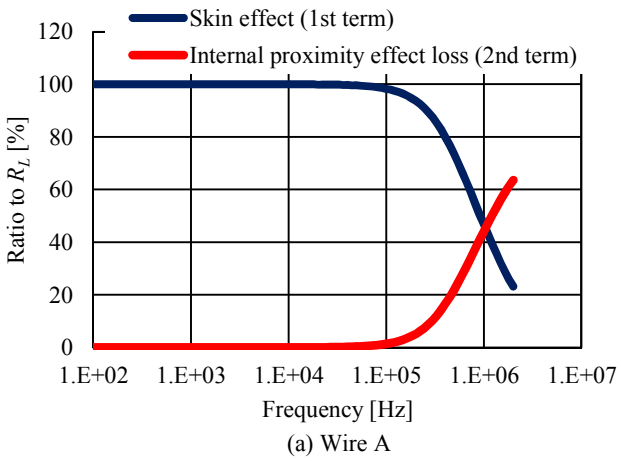

(a) Wire A

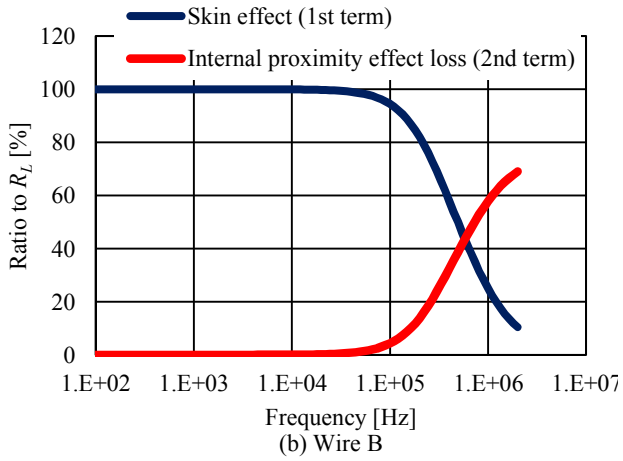

(b) Wire B

Fig. 7. Conposition ratio of the 1st and 2nd terms of equation (31) in the simulation result of R_L.

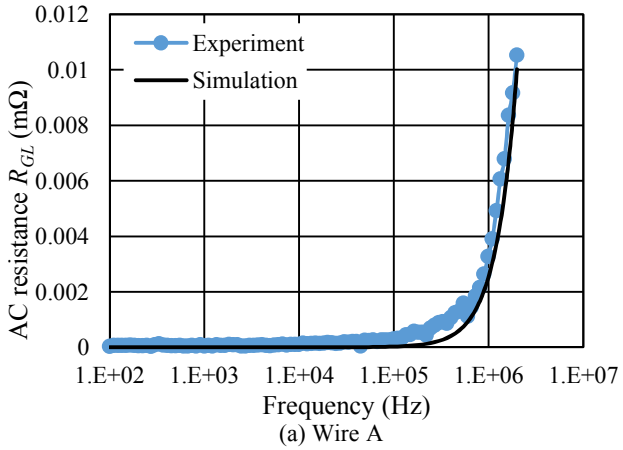

(a) Wire A

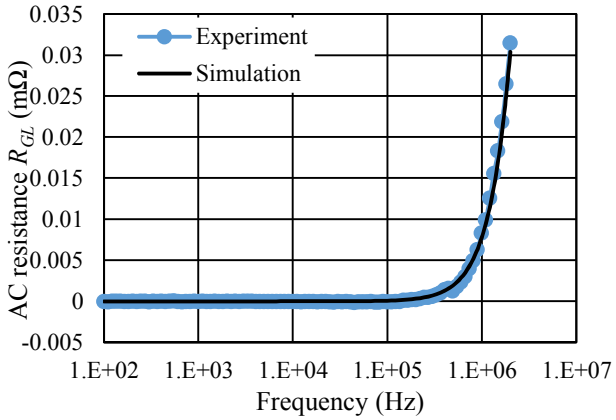

(b) Wire B

Fig. 8. Comparison result between the theoretically predicted R_{GL} and experimentally measured R_{GL}.

which equals the average of the inner and outer radius of the coreless toroid.

The ac magnetic field outside the toroidal Litz wire coil is zero. Therefore, the part of the Litz wire that faces the outside of the toroidal coil has the zero ac magnetic field, whereas the part that faces the inside of the toroidal coil has the ac magnetic field H_{troid}. However, we approximate that the uniform representative external ac magnetic field H_{L_rep} was applied to the Litz wire. We set H_{L_rep} at the RMS average of the ac magnetic field, simply assuming that the ac magnetic field increases linearly from the outer side to the inner side of the Litz wire toroidal coil. Hence, we set

$$H_{L\_rep} = \frac{Ni_L}{2\sqrt{3}\pi r_{eq}}, \tag{34}$$

Consequently, the theoretical value of R_{GL} can be calculated as

$$\begin{aligned} R_{GL} i_L^2 &= G_L H_{L\_rep}^2 = \frac{G_L N^2}{12\pi^2 r_{eq}^2} i_L^2, \\ \therefore R_{GL} &= \frac{G_L N^2}{12\pi^2 r_{eq}^2}. \end{aligned} \tag{35}$$

Figure 6 shows the evaluation results of R_L. The frequency dependence predicted by the proposed model agreed well with the experiment in both of the two experimental Litz wires. According to (31), the coefficient R_L is the sum of the 1st term, which is related to the skin effect inside the Litz wire, and the 2nd term, which is related to the proximity effect caused by the internal magnetic field $\mathbf{H}_{int}$. As can be seen in Fig. 7, which presents the ratio of these two terms to R_L, the 1st term is dominant at low frequencies, whereas the 2nd term is dominant at high frequencies. Therefore, the consistency of R_L between the theory and the experiment for wide frequency range implies appropriateness of both of the 1st and 2nd terms of (31).

Figure 8 shows the evaluation result of R_{GL}. The frequency dependence predicted by the proposed model also agreed well with the experimental result in both of the two experimental Litz wires, although drastic approximation was applied for calculating R_{GL}. As a result, Fig. 8 supported the appropriateness of (32). Consequently, the experiment supported the appropriateness of the proposed model.

IV. Conclusions

The copper loss prediction of the Litz wire is important for design optimization of the Litz wire. However, the Litz wire has the complicated structure with multi-level twisting, which hinders the analytical and numerical analysis of the copper loss. In spite of the difficulty of the fully analytical model of the Litz wire, the preceding studies have long accumulated analytical insights for the loss of the strands and the bundle of twisted strands. Based on these insights, this paper constructed a simple fully analytical copper loss model of the Litz wire. Appropriateness of the proposed copper loss model was evaluated by the experiment. As a result, the proposed copper loss model successfully predicted the

frequency dependence of the ac resistance of the commercial Litz wires, supporting the appropriateness of the proposed model.

REFERENCES

[1] I. Lope, J. Acero, and C. Carretero, "Analysis and optimization of the efficiency of induction heating applications with litz-wire planar and solenoidal coils," *IEEE Trans. Power Electron.*, vol. 31, no. 7, pp. 5089-5101, Jul. 2016.

[2] M. Hataya, Y. Oka, K. Umetani, E. Hiraki, T. Hirokawa, and M. Imai, "Novel thin heating coil structure with reduced copper loss for high frequency induction cookers," in *Proc. IEEE Intl. Conf. Elect. Mach. Syst.* (ICEMS2016), Chiba, Japan, Nov. 2016, pp. 1-6.

[3] M. Hataya, K. Kamaeguchi, E. Hiraki, K. Umetani, T. Hirokawa, M. Imai, and S. Sadakata, "Verification of the reduction of the copper loss by the thin coil structure for induction cookers," in *Proc. IEEE Intl. Power Electron. Conf.* (IPEC2018), Niigata, Japan, May 2018, pp. 410–415.

[4] S. Inoue and H. Akagi, "A bidirectional isolated DC–DC converter as a core circuit of the next-generation medium-voltage power conversion system," *IEEE Trans. Power Electron.*, vol. 22, no. 2, pp. 535-542, Mar. 2007.

[5] W. Shen, F. Wang, and D. Boroyevich, C. W. Tipton IV, "High-density nanocrystalline core transformer for high-power high-frequency resonant converter," *IEEE Trans. Ind. Appl.*, vol. 44, no. 1, pp. 213-222, Jan./Feb. 2008.

[6] W. Water and J. Lu, "Improved high-frequency planar transformer for line level control (LLC) resonant converters," *IEEE Magn. Lett.*, vol. 4, 6500204, Nov. 2013.

[7] E. L. Barrios, A. Ursua, L. Marroyo, and P. Sanchis, "Analytical design methodology for litz-wired high-frequency power transformers," *IEEE Trans. Ind. Electron.*, vol. 62, no. 4, pp. 2103-2113, Apr. 2015.

[8] M. Leibl, G. Ortiz, and J. W. Kolar, "Design and experimental analysis of a medium-frequency transformer for solid-state transformer applications," *IEEE J. Emerg. Sel. Topics Power Electron.*, vol. 5, no. 1, pp. 110-123, Mar. 2017.

[9] C. R. Sullivan and R. Y. Zhang, "Simplified design method for litz wire," in *Proc. IEEE Appl. Power Electron. Conf. Expo.* (APEC2014), pp. 2667-2674, Mar. 2014.

[10] B. A. Reese and C. R. Sullivan, "Litz wire in the MHz range: modeling and improved designs," in *Proc. IEEE Workshop Control Modeling Power Electron.* (COMPEL2018), pp. 1-8, Jul. 2017.

[11] A. Roßkopf, E. Bär, and C. Joffe, "Influence of inner skin- and proximity effects on conduction in litz wires," *IEEE Trans. Power Electron.*, vol. 29, no. 10, pp. 5454-5461, Oct. 2014.

[12] R. Y. Zhang, J. K. White, and J. G. Kassakian, "Fast simulation of complicated 3-D structures above lossy magnetic media," *IEEE Trans. Magn.*, vol. 50, no. 10, pp. 7027416, Oct. 2014.

[13] A. Roßkopf, E. Bär, C. Joffe, and C. Bonse, "Calculation of power losses in litz wire systems by coupling FEM and PEEC method," IEEE Trans. Power Electron., vol. 31, no. 9, pp. 6442-6449, Sept. 2016.

[14] S. Hiruma and H. Igarashi, "Fast 3-D analysis of eddy current in litz wire using integral equation," *IEEE Trans. Magn.*, vol. 53, no. 6, pp. 7000704, Jun. 2017.

[15] J. A. Ferreira and J. D. van Wyk, "A new method for the more accurate determination of conductor losses in power electronic converter magnetic components," in *Proc. 3rd Intl. Conf. Power Electron. Variable-Speed Drives*, 1988, pp. 184-187.

[16] J. A. Ferreira, "Analytical computation of AC resistance of round and rectangular litz wire windings," *IEE Proc. B – Elect. Power Appl.*, 1992, vol. 139, no. 1, pp. 21-25.

[17] M. Bartoli, N. Noferi, A. Reatti, and M. K. Kazimierczuk, "Modeling Litz-wire winding losses in high-frequency power inductors," in *Proc. IEEE Power Electron. Specialists Conf.*, 1996, vol. 2, pp. 1690-1696.

[18] X. Nan and C. R. Sullivan, "An improved calculation of proximity-effect loss in high-frequency windings of round conductors," in *Proc. IEEE Power Electron. Specialists Conf.*, 2003, vol. 2, pp. 853-860.

[19] J. Acero, R. Alonso, J. M. Burdio, L. A. Barragan, D. Puyal, "Frequency-dependent resistance in litz-wire planar windings for domestic induction heating appliances," *IEEE Trans Power Electron.*, vol. 21, no. 4, pp. 856-866, Jul. 2006.

[20] J. Acero, R. Alonso, J. M. Burdio, L. A. Barragan, C. Carretero, "A model of losses in twisted-multistranded wires for planar windings used in domestic induction heating appliances," in *Proc. IEEE Appl. Power Electron. Conf. and Expo.*, 2007, pp. 1247-1253.

[21] X. Nan and C. R. Sullivan, "An equivalent complex permeability model for litz-wire windings," *IEEE Trans. Ind. Appl.*, vol. 45, no. 2, pp. 854-860, Mar./Apr. 2009.

[22] D. Sinha, P. K. Sadhu, N. Pal, and A. Bandyopadhyay, "Computation of inductance and AC resistance of a twisted litz-wire for high frequency induction cooker," in *Proc. Intl. Conf. Ind. Electron. Control Robotics*, 2010, pp. 85-90.

[23] R. P. Wojda and M. K. Kazimierczuk, "Winding resistance of litz-wire and multi-strand inductors," *IET Power Electronics*, vol. 5, no. 2, pp. 257-268, Jan. 2012.

[24] V. Väisänen, J. Hiltunen, J. Nerg, and P. Silventoinen, "AC resistance calculation methods and practical design considerations when using litz wire," in *Proc. Annu. Conf. IEEE Ind. Electron. Soc.* (IECON2013), 2013, pp. 368-375.

[25] C. R. Sullivan and R. Y. Zhang, "Analytical model for effects of twisting on litz-wire losses" in *Proc. IEEE Workshop Control Modeling Power Electron.* (COMPEL), 2014, pp. 1-10.